

Full Length Research Paper

Fourier transform infrared spectroscopic characterization of clay minerals from rocks of Lalibela churches, Ethiopia

Alemayehu Kiros^{1*}, A. V. Gholap¹ and Giovanni E. Gigante²

¹Department of Physics, Faculty of Science, Addis Ababa University, P. O. Box -1176, Addis Ababa, Ethiopia.

²La Sapienza University, Rome, Italy.

Accepted 16 January, 2013

This study demonstrates the Fourier transform infrared (FTIR), Raman spectroscopy and scanning electron microscope - energy dispersive X-ray spectrometer (SEM-EDS) techniques which has been applied to characterize decay products and processes occurring at the surface of rock-hewn churches at the UNESCO's World Heritage site of Lalibela, Northern Ethiopia. Spectroscopic analyses comparing the observed frequencies with the available literature, minerals were identified. A special emphasis is devoted to the presence of whewellite/weddellite and kaolinite minerals, never pointed out before this study in the rock hewn churches of Lalibela, and their possible roles on rock decay. The identification of montmorillonite as a weathering product up to 20 mm from the rock/atmosphere interface beyond the level at which kaolinite, whewellite and gypsum are found, suggests that montmorillonite may penetrate even deeper into the rock substrate causing major rock decay. Results indicate that biological attack by green algae and lichens is currently responsible for severe stone surface, physical and chemical weathering leading to considerable weakening of the churches walls. A prompt and careful removal of the biological and other deposits with the non-destructive method (laser cleaning) treatment is therefore recommended.

Key words: Fourier transform infrared (FTIR), Raman, whewellite, kaolinite, rock hewn churches, mineral characterization.

INTRODUCTION

Lalibela is known throughout the world for its extraordinary complex of 11 monolithic churches (Figure 1), carved, some 800 years ago during the Empire of King Lalibela. The main cluster of 11 churches is located in the middle of the village since 1978; the churches and their surrounding area have been included in UNESCO's World Heritage List (Asrat and Ayallew, 2011). Water absorption represents the main contributing factor of damage for high exposed rock materials and structures, in terms of direct rainfall, soil infiltration, capillarity and diffuse humidity, for the alteration of basalt (Delmonaco et al., 2009). Another study (Asrat and Ayallew, 2011) reported material loss due to deep weathering activated

by rain water penetration and the leakage of groundwater affects most of the Lalibela churches. This exposure has resulted in the severe degradation of the churches, most of which are now considered to be in a critical condition. A first restoration attempt of the Lalibela rock-hewn churches was carried out in 1920 (Delmonaco et al., 2009). Currently, most of the churches are protected by shelters to prevent the erosive effects of rainfall, especially on the roof rock cover, and temporary scaffolding to prevent collapse of the most exposed structures.

In many cases, the presence of biological colonization by lichens and other major plants is quite evident. For the study of biological aspects of weathering of rocks and minerals, lichen-encrusted rocks provide an ideal environment. The effects of lichens on their mineral substrates can be attributed to both physical and chemical processes. Lichens also have significant impact

*Corresponding author. E-mail: ftkiros@gmail.com. Tel: +251911863347. Fax: +251111223931.



Figure 1. Lalibela location map. Inlet (top right) shows the geographical distribution of the rock-hewn churches at the Lalibela monumental site.

in the chemical weathering of rocks by the secretion of various organic acids, particularly oxalic acid, which can effectively dissolve minerals and chelate metallic cations (Adamou and Violante, 2000; Chen et al., 2000). As a result of the weathering induced by lichens, many rock-forming minerals exhibit extensive surface corrosion.

Raman spectroscopy, scanning electron microscope - energy dispersive X-ray spectrometer (SEM-EDS) and Fourier transform infrared (FTIR) techniques found many applications in the field of geology, archaeology and cultural heritage analysis due to its non-invasiveness. The infrared spectroscopic investigation is found to be an ideal tool for structure elucidation and for estimating quartz crystallinity of the natural samples (Saikia et al., 2008), and characterization of natural kaolinite (Saikia and Parthasarathy, 2010). FTIR and EDS are established tool for the ceramic body identification (Ravisankar et al., 2010), to study the ancient potteries (Ravisankar et al., 2010; Ravisankar et al., 2012). FTIR is also a reliable method for the characterization of the organic matter preserved in carbonates, and generally in all types of sedimentary rocks (Ravisankar et al., 2010; Schiavon, 2007). Raman spectroscopy and micro-Raman study provides a tool for examination of building stones, and is

particularly useful for the investigation of surface degradation (Perez-Alonso et al., 2004; Potgieter-Vermaak et al., 2005).

Clay mineral characterization could be carried out employing spectroscopic methods for various purposes in the building stones (Schiavon, 2007; Davarcioglu and Ciftci, 2010). In the present work, we report and discuss the experimental results obtained through FTIR transmittance, Raman spectroscopy and EDS measurements performed on rock samples to report qualitative and quantitative data for the deleterious components of the rock hewn churches of Lalibela. Our previous X-ray diffraction (XRD) data on whole rock samples confirm the presence of peaks attributable to zeolites (in order of peak strength: analcime, heulandite, thomsonite, wairakite, pollucite, clinoptilite, scolecite), clinopyroxene, hematite, calcite, magnetite and minor smectites.

Climatic and geological setting

The Lalibela area has two rainy seasons from June to September and from March to April. The annual rainfall



Figure 2. Sampling sites. Bete Giyorgis with widespread lichenous cover and Bete Mikael Golgotha with widespread green algae and black crust cover.

varies from 500 to 1000 mm, which is believed to be the main direct/indirect cause of stone deterioration (Smith et al., 2008; McCabe et al., 2011). Lalibela area is characterized by mean annual temperature of 24.5°C and relative humidity is 52.9% (Asrat and Ayallew, 2011; Delmonaco et al., 2009).

Northern Ethiopia's geology is characterized by thick sequences of tholeiitic to transitional continental flood basalts overlain by minor rhyolitic-trachytic lavas and pyroclastic rocks of Oligocene to Miocene belonging to the Northern Ethiopia Plateau (Beccaluva et al., 2009; Natali et al., 2011; Asrat and Ayallew, 2011). Within the plateau, three magma types have been distinguished: two high-titanium (Ti) groups (HT1 and HT2), and one low-Ti group (LT). The central-eastern sector of the plateau in particular, that is, the one comprising the Lalibela area and facing the Afar triangle, is mainly characterized by a 1700 m-thick sequence of high TiO_2 (HT2 magma type) picrite/basalt lavas capped by about 300 m of rhyolites, linked to the magmatic activity at the Afar plume axial zone (Beccaluva et al., 2009). The HT2 volcanics (Pik et al., 1998) are represented by sub-alkaline olivine-clinopyroxene aphyric or glomerophytic basalts and picrites with phenocrysts of euhedral olivine (FO_{86} - FO_{81} range) and of Mg-Ti-Al rich augite. The ground mass contains olivine, clinopyroxene, Fe-Ti oxides and plagioclase (An85-An48 range) microlites. The Oligocene volcanism of the northwestern Ethiopian Plateau has been subdivided into three formations (Berhe et al., 1987); the Ashangi and Amba Aiba basaltic units, separated by an angular unconformity (Zanettin, 1992) from the upper ignimbritic Alaji unit. In the Lalibela monumental site, the Amba Aiba basalts are typically

overlain by a thick horizon of reddish highly hydrothermally weathered basaltic scoria (commonly referred to as "tuffaceous material"). It is within this "softer" unit that the rock-hewn churches were carved.

MATERIALS AND METHODS

Samples were collected from internal and external walls of three Lalibela churches: Bete Michael Golgotha-external (BM-R; Figure 2), Bete Giyorgis-external (BG-E; Figure 2), Bete Gebriel-Rufael-internal (BR-I), Bete Giyorgis Mahilet (BGM-B, BGM-R; Figure 3) and tunnel from Bete Gabriel to Bete Merkorios (TG-M). For comparison and depth profiling analysis, we also performed the measurements on two rock samples from the surrounding: one from the tunnel in front of Bete Amanuel, bulk tuff weathered (Ts) and bulk tuff lateral cut (T4) and the other one collected on the north side of Bete Giyorgis, bulk basalt weathered (Bs) and bulk basalt lateral cut (B4) (Figure 3). The samples were submitted for analyses according to the specific requirements of the following analytical techniques: SEM-EDS, FTIR, μ -Raman and Raman spectroscopy.

In FTIR spectroscopy, samples are exposed to IR radiation and a fraction of the IR radiation is absorbed at wavelengths that are specific to the molecular excitation states of covalently bonded atoms. Each molecule has its own specific absorption spectrum, and the IR spectra are represented as a plot of transmittance across the IR band. A portion of rock samples was pulverized to a fine powder in an agate mortar and pestle. A small portion of the material weighing approximately 2 mg was then ground and mixed thoroughly with 40 mg of dried potassium bromide (KBr). The powder was distributed evenly within the die by first rotating the plunger, and the assembly was placed in a press. A load of 10 tones was applied for 3 to 4 min to form a transparent KBr disc. The die was disassembled and the disc carefully removed and placed in a sample holder. The Perkin Elmer Spectrum 65 Spectrum BX FTIR (at Addis Ababa University, Department of chemistry, Ethiopia) was used. The beam splitters used were KBr for the mid-IR region 4000

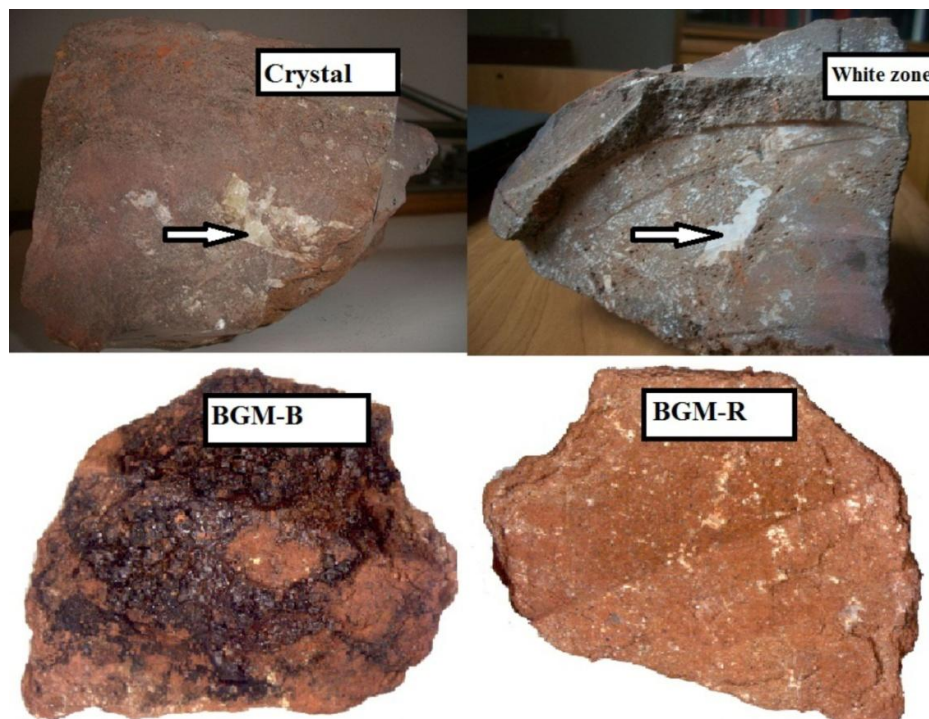


Figure 3. Bulk samples from rock hewn churches of Lalibela: basalt(surface) the arrow indicates the analyzed crystal using Raman, basalt(lateral cut) the arrow indicates the analyzed white zone using Raman and Bete Giyorgis Mahilet-Black (BGM-B), Bete Giyorgis Mahilet-Red (BGM-R) analyzed using FTIR.

to 400 cm^{-1} and the resolution was 4 cm^{-1} . The moving mirror velocity 0.6 cm/s and bi-directional Interferogram were used. For room-temperature measurements, we used Mercury Cadmium Telluride (MCT) detector for mid-IR spectra.

Micro-Raman characterization was performed using a Renishaw 2000 μ -Raman instrument equipped with a Peltier refrigerator-cooled charge-coupled device (CCD) camera in conjunction with a Leica optical microscope at CNR, Institute for the Study of Nanostructure Materials Research Area of Rome 1- Monte libretti - Italy. The laser was focused on the sample through a $\times 100$ or $\times 50$ objective lenses. The excitation light was the 514.5 nm line of an Ar^+ laser and a 785 nm line of a diode laser with laser power in the range of 10 to $60\text{ }\mu\text{W}$. Care was taken to avoid sample damage and the typical spectrometer resolution was about 2 cm^{-1} .

Measured spectrum of calcite on the crystal and white area (Figure 3) of basalt rock is qualitatively determined by using Avantes AvaRaman-532 TEC Raman instrument equipped with a TE cooled AvaSpec-2048TEC-USB2 Spectrometer with 1200 lines/mm grating set of 535 to 752 nm , $25\text{ }\mu\text{m}$ slit, DCL-UV/VIS at (La Sapienza University, Department of Physics Rome). The excitation light was the 532 nm line of solid state laser with laser power of 50 mW , and FWHM 0.2 nm . The instrument scanned the spectra 10 times in integration time of 3 s .

SEM-EDS micro-morphological and chemical investigations were carried out by a Cambridge 360 SEM, equipped with a LaB_6 filament at CNR, Institute for the Study of Nanostructure Materials Research Area of Rome 1 - Monte libretti - Italy. Images with a higher spatial resolution were obtained by a high brilliance LEO 1530 field emission-SEM (FE-SEM) apparatus. Both the SEM and FE-SEM instruments were equipped with an EDS, INCA 250 and INCA 450, respectively, and a four sectors backscattered electron detector (BSD). SEM images were recorded both in the secondary

electron image (SEI) and BSD image mode at an acceleration voltage at 20 kV . FE-SEM images were recorded both in SEI and BSD mode at different acceleration voltage ranging from 20 to 3 kV . Samples were coated with a thin layer of carbon or chromium in order to avoid charging effects. The carbon coating was deposited by using an Emitech sputter coater K550 unit, a K 250 carbon coating attachment and a carbon cord at a pressure of $1 \times 10^{-2}\text{ mbar}$ in order to produce a carbon film with a constant thickness of about 3.0 nm . The chromium coating was deposited by using a Bal-Tech SCD 500 equipped with turbo pumping for ultra clean preparations at a pressure of $5 \times 10^{-3}\text{ mbar}$ in order to produce a chromium film with a constant thickness of about 0.5 nm .

RESULTS AND DISCUSSION

FTIR results are summarized in Tables 1 and 2 where a series of analytical values wavenumber (in cm^{-1}) of the absorption bands of FTIR spectra of the powder samples are taken from the bulk tuff, bulk basalt and from internal and external walls of rock hewn churches of Lalibela. A typical example of FTIR spectra of surface crusts and in depth profile are shown in Figure 4. FTIR analysis comparing the observed frequencies with the available literature, secondary minerals such as calcite, kaolinite, whewellite, montmorillonite, gypsum, magnetite and hematite was identified.

FTIR spectrum obtained on the basalt samples are shown in Figure 4. The characteristic bands of calcite are

Table 1. Absorption frequency in the region of 4000 to 400 cm^{-1} of the bulk basalt and bulk tuff of Lalibela, together with minerals identification.

Sample	Kao	Mont	Cal	Gy	Hm	Mg	Ww	Wd
Bs	3694	3427	2514					
	3619	1642	1799					
	1031		1421	-	-	-	1320	-
	444		876					
			712					
B4	1032	3435	2513					
	438	1628	1799					
			1421	-	-	-	-	-
			876					
			711					
Ts	3677			3541				
	1034			3406				
				1671				
		1637	-	1622	540	582	1311	1355
				1140				
				1116				
				670				
			603					
T4	1043	3434 1638	-	-	539	578	-	-

Bs, Bulk basalt surface; B4, bulk basalt 20 mm deep; Ts, bulk tuff surface; T4, bulk tuff 20 mm deep; Kao, Kaolinite; Mont, Montmorillonite; Cal, calcite; Gy, gypsum; Hm, hematite; Mg, Magnetite; Ww, whewellite; Wd, Weddellite.

present, the sharp one at 876 cm^{-1} , is due to its asymmetric bending. Calcite FTIR spectrum shows (Table 1) peaks at 1424 to 1421, 876 and 712 to 711 cm^{-1} due to the C–O stretching of carbonate, and the weak peaks at 1799 and 2514 to 2512 cm^{-1} , which are combination and overtone bands (Gunasekaran and Anbalagan, 2008; Ravisankar et al., 2012; Ravisankar et al., 2010; Hans and Adler-Paul, 1962; Makreski and Jovanovski, 2003; Plav et al., 1999; Larson and Kerr, 1963). Hematite shows the characteristic peaks at 536 to 544 cm^{-1} (Ravisankar et al., 2010; Ravisankar et al., 2012), magnetite is related to 579 to 583 cm^{-1} peak.

The gypsum spectrum at $\nu = 3547$, and 3407 cm^{-1} (OH stretching), 1685, and 1622 cm^{-1} (O–H–O bending of the crystallization water) and at 670 cm^{-1} corresponding to the sulphate ions (Lane, 2007; Schiavon, 2007). The representative of gypsum at $\nu = 670 \text{ cm}^{-1}$ shows only on the surface of weathered tuff (bulk), in samples collected from BR-I, BG-E and TG-M.

Among the oxalates are the two calcium oxalates known as weddellite and whewellite. The secondary carbonyl stretching band, the metal-carboxylate stretch, ν_s (COO-), is located at 1322 cm^{-1} for whewellite and at 1355 cm^{-1} for weddellite (Ruffolo et al., 2010; Hernanz

etal., 2006; Kuzmanovski et al., 1999; Sofia et al., 2010; Manjula et al., 2012; Frost et al., 2003; Valarmathi et al., 2010). The characteristic feature of whewellite at $\nu = 1322 \text{ cm}^{-1}$ shows weak and weddellite at $\nu = 1355 \text{ cm}^{-1}$ is very weak.

The most characteristic spectrum of montmorillonite is the broad absorption band that varies from 3300 to 3500 cm^{-1} . Usually, this band centered at about 3400 cm^{-1} is due to stretching of the O–H molecule of water present in the interlayer region of montmorillonite (Madejova and Komadel, 2001). From Tables 1 and 2, the presence of peaks at 3435 to 3427 and 1642 to 1628 cm^{-1} in all samples indicates the presence of montmorillonite, as reported by many workers (Ravisankar et al., 2010; Saikia and Parthasarathy, 2010; Ravisankar et al., 2012). The characteristic spectrum of montmorillonite at $\nu = 3435 \text{ cm}^{-1}$ is only present in samples BG-E, BM-R and bulk samples (basalt, tuff).

Kaolinite shows a sequence characteristic IR absorption in the range of 3700 to 3600 cm^{-1} . The peak at $\nu = 3694 \text{ cm}^{-1}$ is due to OH stretching frequencies associated with the hydroxyl and the band observed at approximately 3620 cm^{-1} for kaolinite is as a result of an inner hydroxyl stretch (Madejova and Komadel, 2001;

Table 2. Absorption Frequency in the region of 4000 to 400 cm^{-1} of the samples collected from internal and external walls of rock hewn churches of Lalibela, together with minerals identification.

Sample	Kao	Mont	Gy	Hm	Mg	Ww	Wd
TG-M	1035	1638	3410				
	1016	520	674	-	579	-	-
	448		603				
BR-I	3676		3538				
	1031		3406				
			1622				
		-	1685	-	579	1326	1354
			1115				
			671				
			602				
BG-E	1032	3427	3415	536	583	1324	-
	444	1632	670				
BM-R	1035	3434	-	-	580	1315	1356
	445	1639					
BGM-B	3681		3533				
	1039	1643	3401	533	-	1322	-
	444						
BGM-R	1040	1639	3534	540	-	1323	-
	444		3408				

TG-M, Tunnel from Bete Gebriel to Bete Merkorios; BM-R, Bete Mikeal Golgota-Right; BG-E, Bete Giyorgis-External; BR-I, Bete Gebriel Rufael; BGM-B, Bete Giyorgis Mahilet-Black; BGM-R, Bete Giyorgis Mahilet-Red; Kao, Kaolinite; Mont, Montmorillonite; Cal, calcite; Gy, gypsum; Hm, hematite; Mg, Magnetite; Ww, whewellite; Wd, Weddellite.

Farmer, 1998). This inner hydroxyl group results from bonding between a proton and an oxygen that is also coordinated to Al^{3+} in an octahedral site. The IR absorption peaks appear at 3694, 3619, 1040 to 1043, 1031 to 1034, 1016 to 1023 and 438 to 444 cm^{-1} in the samples as reported (Saikia and Parthasarathy, 2010; Ravisankar et al., 2012; Davarcioglu and Ciftci, 2010; Ravisankar et al., 2010; Schiavon, 2007; Madejova and Komadel, 2001; Farmer, 1998), which indicates the presence of kaolinite (Tables 1 to 2). The characteristic feature of kaolinite appear only on the surface of the weathered basalt (Bs), very weak at $\nu = 3694 \text{ cm}^{-1}$.

Raman spectroscopy revealed the bands of mineral at the surface of samples basalt, the crystal on the surface (Figure 3) and the white zone on the surface of basalt (lateral cut) (Figure 3), and the absorption intensity of the samples are compared with the reference samples, marble and quartz (Figure 5). The peak intensities of the samples are highly associated with the marble reference sample at peak intensities 713, 1077 and 1428 cm^{-1} . The intense band (ν_1) of calcite spectrum corresponds to the

symmetric stretching of CO_3 group at 1077 cm^{-1} . The ν_2 (asymmetric deformation) vibration mode is not active in Raman. The values attributed to ν_3 (asymmetric stretching) mode are 1428 cm^{-1} and ν_4 (symmetric deformation) mode at 706 cm^{-1} (Gunasekaran and Anbalagan, 2008; Edwards et al., 2000). The band intensity of the crystal shows higher than the white area, whereas the FTIR analysis show higher in the sample B4 (lateral cut); it is perhaps during sample preparation, high concentration of calcite were taken from basalt (lateral cut) in the FTIR analysis.

Micro Raman on the tuff sample confirmed the extensive laterization experienced by the basaltic pyroclastic scoria deposit with the identification (beside peaks attributable to zeolitic (analcime) minerals) of well-defined peaks of hematite, lepidocrocite and combined hematite/lepidocrocite (Figure 6). The positions of the hematite spectral peaks are shown at 227, 293, 409, 499, and 609 cm^{-1} (Franquelo et al., 2009). According to Edwards et al. (2000), the Raman spectrum of lepidocrocite ($\gamma\text{-FeOOH}$) exhibits a broad band

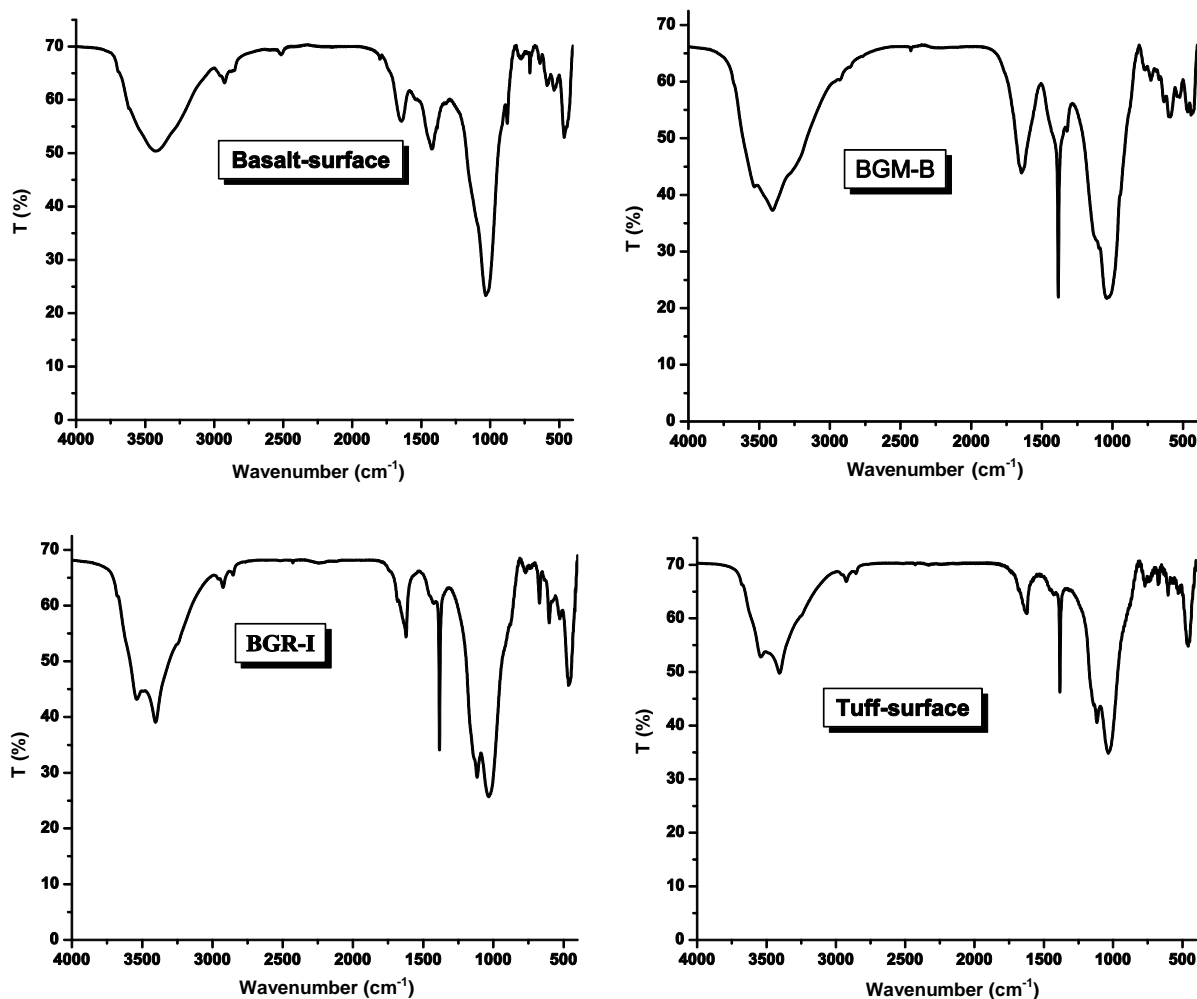


Figure 4. FTIR spectrum of the rock samples taken from the bulk basalt surface, bulk tuff surface, Bete Gebriel Rufael-internal (BGR-I) and Bete Giyorgis Mahilet-Black (BGM-B).

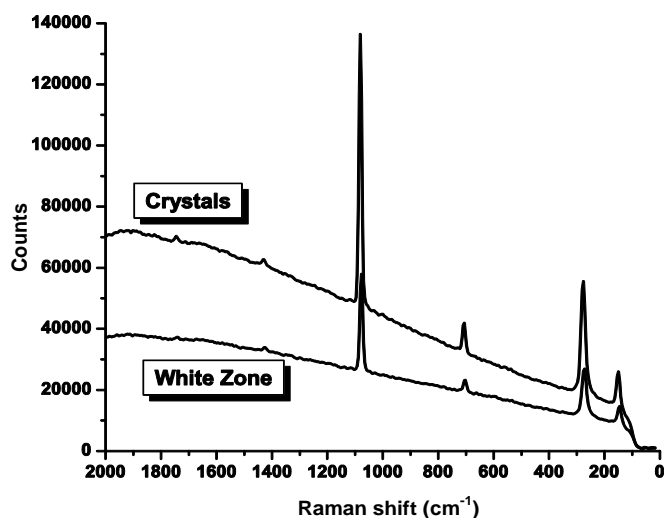


Figure 5. Raman spectrums of the rock samples taken from the crystal (Bs) and white zone (B4) bulk basalt.

about 1312 cm^{-1} .

The SEM-EDS major elements composition of the samples representing BG-M, tuff and basalt of the rock hewn churches of Lalibela are given in Table 3. All samples contain Carbon (C), Oxygen (O), Magnesium (Mg), Aluminium (Al), Silicon (Si), Potassium (K), Calcium (Ca), Titanium (Ti) and Iron (Fe). Samples BG-M and tuff also contain detectable levels of Na and P, while sample BG-M contain S. Coarse differences in composition are clear between the sample basalt and the others. Sample basalt appears to be particularly C and Ca rich, sample tuff contain high quantity of Na, sample BG-M contains more Fe and S than the other samples. The nature of these compositional differences can be investigated further through the individual element maps and the results of targeted area analysis of different surface chemical phases. The Mg value ranges between 1.98 to 3.06%, while Ca content varies between 5.11 to 14.2%, Si and Fe concentrations range from

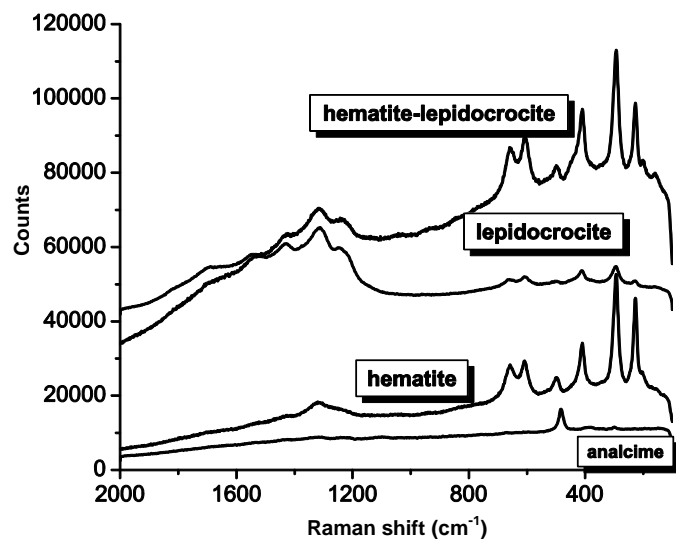


Figure 6. Raman spectrum of bulk tuff, collected from rock hewn churches of Lalibela.

10.99 to 13.43% and from 6.21 to 15.32%, respectively. From the EDS analysis, the abundant amount of Si, Al, Ca, Mg, Fe, K and Ti was found and it supports the vibrational spectroscopic findings; the presence of aluminosilicates (Si, O, Al, K, Na, Mg), Fe-rich oxide (Fe–O) and gypsum (Ca–S–O) (Ravisankar et al., 2010).

FTIR spectroscopy, Raman spectroscopy and EDS analysis result confirms that the Lalibela churches were widespread, abundant presence within the stone fabric of secondary minerals belonging to the zeolite, smectite (montmorillonite), kaolinite, whewellite/weddellite, hematite, lepidocrocite, calcite and gypsum has surely had important bearings on the stone susceptibility to weathering.

The presence of montmorillonite and analcite are reported by other workers (Delmonaco et al., 2009; Renzullia et al., 2011) as the sources of the progressive deterioration of the geomechanical properties of the rocks in Lalibela. In the present study, we bring attention to the presence of kaolinite, gypsum and whewellite/weddellite not identified before on the rock hewn churches of Lalibela, besides the presence of montmorillonite in depth of bulk samples.

The presence of lower amounts of olivine phenocrysts have been detected as compared with typical Ethiopian HT2 basalts and indeed no peaks unequivocally ascribable to olivine have been found in the FTIR analyses: this can be due to the highly hydrothermally altered nature of the olivine crystals that are often almost completely altered (laterized) to secondary Fe-rich oxide-hydroxides [hematite, magnetite and lepidocrocite (γ -FeOOH)]. The presence of Fe-rich oxide-hydroxides in the rock samples were evidenced by μ -Raman (Figure 6) and SEM-EDS (Table 3). In the most highly weathered sample BGM-B (Figure 3), the texture of the original

Table 3. Elemental composition of rock samples of Rock hewn churches of Lalibela (Mean % weight).

Element	BGM	Basalt	Tuff
C	9.71	13.35	11.02
O	43.77	45.62	45.27
Na	1.70	-	2.79
Mg	3.06	1.98	2.23
Al	3.90	3.01	4.86
Si	12.33	10.99	13.43
P	0.78	-	0.78
S	1.17	-	-
K	2.50	3.45	0.56
Ca	6.33	14.2	5.11
Ti	2.65	1.79	2.1
Fe	15.32	6.21	11.84

BGM, Bete Giyorgis Mahilet.

basalt has been completely destroyed and the bulk of the rock is an intimate mixture of clay and hematite (Figure 7).

The identification of specific zeolite, in the Raman analyses should help to distinguish hydrothermal alteration in the Lalibela rocks. These minerals have a great ability to reversibly adsorb and desorb water molecules as a function of temperature and/or humidity. The potential role of the zeolite in the decay processes of the Lalibela architectural complex should be taken into account and considered as one of the main stone basic causes (Delmonaco et al., 2009).

Among the highly active in synergistically causing severe degradation in the rock hewn churches of Lalibela are: microbial biofilms which more than often act as precursors to the subsequent development of stone surface covering lichenous mats and are widespread in Lalibela, modify the capillary water uptake of porous stone material causing measurable alterations in the water-vapor diffusion properties of the lithic material. Furthermore, the water and moisture retention properties of the lichen patinas may enhance physical decay stresses associated with naturally occurring freeze-thaw cycles. In urban environments, biofilms have also been found to enhance the dry/wet deposition of atmospheric gaseous and particulate pollutants on outdoor stone facades (Schiavon, 2007) thus, playing a role in the bio-mediated precipitation of sulphate compounds such as gypsum and providing an additional route for salt weathering decay and growth of surface weathering black crusts. Field experience has suggested that in the Lalibela monumental site, wood burning and/or solid waste are the major issue in the area exhaust emissions-linked air pollution. The calcite identified by FTIR analysis in the basalt sample is also confirmed by the Raman, XRD and SEM-EDS analysis. The high peak of calcite may be due to the reaction of CO_2 with Ca oxides.

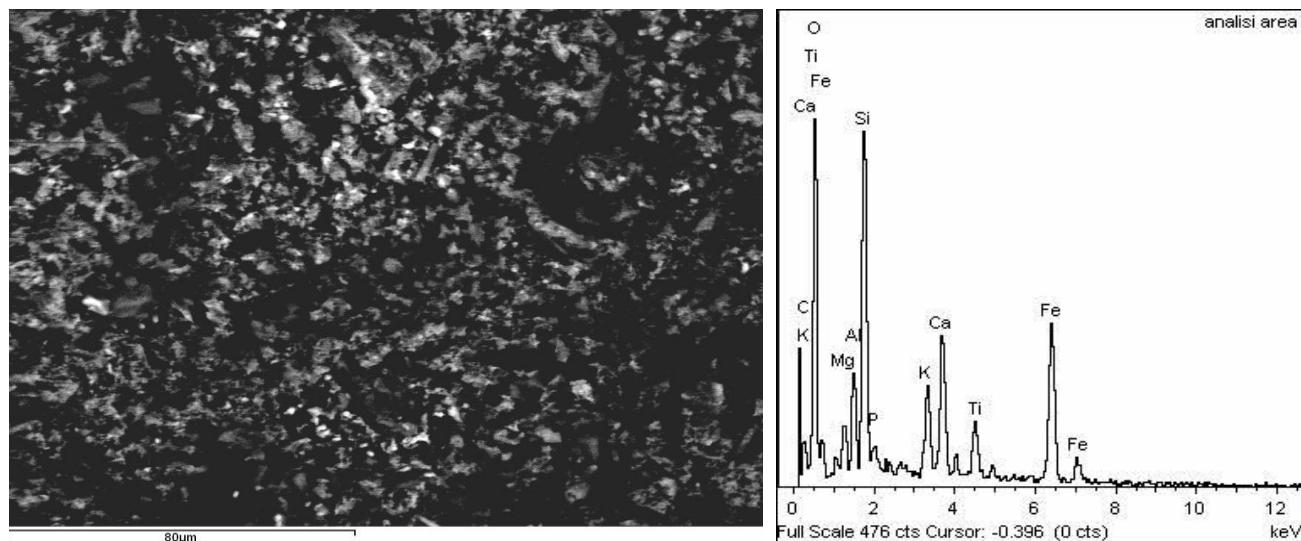
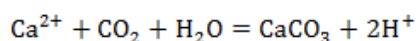
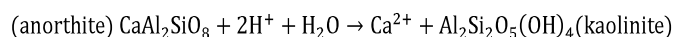


Figure 7. SEM photomicrographs with related EDS spectra, intimate mixture of clay (white) and hematite (black) in red weathered sample of the rock-hewn churches Bete Giyorgis Mahilet-Black (BGM-B).

This oxide is prevalent in silicate minerals.



In the FTIR and XRD analysis, Ca- plagioclase (anorthite) is not identified in basalt sample. Neutralization of H^+ will take place by reaction with the primary mineral phases in the basaltic host rock, as simplified in reaction below. Plagioclases are always replaced by kaolinite.



Kaolinite is a non-swelling clay mineral; it does not have a permanent negative charge and therefore has no exchangeable cations present in the interlayer. The kaolinite found on samples of basalt stone could have the origin: deposition of kaolinite bearing airborne soil dust and/or surface wash on the monument surface and natural weathering in the original basalt stone, such as organic acids excretion by the mycobiont of lichens. Lichens enhance the rate of dissolution of plagioclase (Steven, 2005).

Biogeochemical weathering also plays a major role in the deterioration of the volcanic stone in the Lalibela monuments, acidolysis/dissolution and metal complexation (Adamou and Violante, 2000; Chen et al., 2000). The excretion by the mycobiont of lichens of low molecular weight organic carboxylic acids, such as oxalic, citric, gluconic, lactic acids, with combined chelating and acidic properties, and the production of slightly water soluble polyphenolic compounds called "lichen acids", are processes known to lead to the formation of complexes with the metal cations (such as Mg^{++} and Fe^{++}) in the rock-forming minerals, eventually leading to their extraction by

chelation to be used as nutrients and energy suppliers by green algae and lichen organisms (Adamou and Violante, 2000; Chen et al., 2000). In Lalibela, oxalate compounds (that is, whewellite/weddellite), have only rarely been detected by FTIR analysis.

The variation in intensity values along the weathering depth profile of the bulk samples for selected absorption bands, are chosen as representative of kaolinite (3694 cm^{-1}), gypsum (670 cm^{-1}), montmorillonite (3427 to 3435 cm^{-1}), and whewellite (1311 to 1328 cm^{-1}). The bands of kaolinite, gypsum and whewellite only appear on the surface of the bulk rocks (Tables 1 to 2). Montmorillonite band at 3427 to 3435 cm^{-1} shows a different trend in depth profile of FTIR analysis from the bulk tuff and basalt (that is, from surface down to unweathered tuff and basalt substrate with 5 mm difference). The identification of montmorillonite as a weathering product up to 20 mm from the rock/atmosphere interface beyond the level at which kaolinite, gypsum and whewellite are found suggests that montmorillonite may penetrate even deeper into the rock substrate causing major rock decay. The presence of swelling montmorillonite could result from surface weathering or hydrothermal alteration, minor dissolution-crystallization processes of soluble salts and the whole inexorable lateritization processes, typical of regions with dry and rainy seasons, are all consistent with the deterioration of the rocks of Lalibela.

Conclusion

The qualitative identification of minerals in the rock samples was carried out by FTIR, XRD, and Raman spectroscopy techniques. The spectroscopic analyses of rock samples from the rock hewn churches of Lalibela

indicate the presence of secondary minerals zeolite-group, calcite, kaolinite, whewellite/weddellite, montmorillonite, gypsum, magnetite, lepidocrocite and hematite. Among the different secondary minerals, montmorillonite is present more or less in all samples, however, gypsum and calcite, were the most abundant minerals in samples tuff (Ts), BR-I and bulk basalt, respectively. The high presence of calcite in the sample basalt (bulk) is also confirmed by Raman spectroscopy techniques.

According to the Department of Authority for Research and Conservation of Cultural Heritage (ARCCH), Ethiopia, deposits like lichens and green algae were removed from the churches using mechanical method. The use of rotating abrasive discs or brushes is normally not advisable because they are both inefficient and damaging. Currently, most of the churches are protected by shelters to prevent the erosive effects of rainfall, especially on the roof rock cover, and temporary scaffolding to prevent collapse of the most exposed structures. Results indicate that biological attack by green algae and lichens is currently responsible for severe stone surface, physical and chemical weathering leading to considerable weakening of the churches walls. A prompt and careful removal of the biological and other deposits with the non-destructive method (laser cleaning) treatment is therefore recommended, together with understanding of the indicators of climatic and environmental change (Smith et al., 2008; McCabe et al., 2011).

REFERENCES

- Adamou P, Violante P (2000). Weathering of rocks and neogenesis of minerals associated with lichen activity. *Appl. Clay Sci.* 16:229-256.
- Asrat A, Ayallew Y (2011). Geological and geotechnical properties of the medieval rock hewn churches of Lalibela, Northern Ethiopia. *Afr. J. Earth Sci.* 59:61-73.
- Beccaluva L, Bianchini G, Natali C, Siena F (2009). Continental flood basalts and mantle plumes: A case study of the Northern Ethiopian Plateau. *J. Petrol.* 50(7):1377.
- Berhe SM, Desta B, Nicoletti M, Teferra M (1987). Geology, geochronology and geodynamic implications of the Cenozoic magmatic province in W and SE Ethiopia. *J. Geol. Soc. London* 144:213.
- Chen J, Blume HP, Beyer L (2000). Weathering of rocks induced by lichen colonization: A review. *Catena* 39:121-146.
- Davarcioğlu B, Ciftçi E (2010). The clay minerals observed in the building stones of Aksaray Guzelyurt area (Central Anatolia-Turkey) and their effects. *Int. J. Phys. Sci.* 5(11):1734-1743.
- Delmonaco G, Margottini C, Spizzichino D (2009). Analysis of rock weathering and conservation strategies for rock-hewn churches of Lalibela (Ethiopia). In *Protection of Historical Buildings, PROHITECH 09* ed. Mazzolani (ed). Taylor & Francis Group, London. pp. 137-142.
- Edwards HGM, Newton EM, Russ J (2000). Raman spectroscopic analysis of pigments and substrata in prehistoric rock art. *J. Mole. Struct.* pp. 550-551, 245-256.
- Farmer VC (1998). Differing effects of particle size and shape in the infrared and Raman spectra of kaolinite. *Clay Miner.* 33:601-604.
- Franquelo ML, Duran A, Herrera LK, Jimenez MC, Perez-Rodríguez JL (2009). Comparison between micro-Raman and micro-FTIR spectroscopy techniques for the characterization of pigments from Southern Spain Cultural Heritage. *J. Mole. Struct.* pp. 924-926, 404-412.
- Frost RL, Yang J, Ding Z (2003). Raman and FTIR spectroscopy of natural oxalates: Implications for the evidence of life on Mars. *Chi. Sci. Bull.* 48(17):1844-1852.
- Gunasekaran S, Anbalagan G (2008). Spectroscopic study of phase transitions in natural calcite mineral. *Spectrochim. Acta.* 69:1246-1251.
- Hans H, Adler-Paul FK (1962). Infrared study of Aragonite and Calcite. *Am. Miner.* P. 47.
- Hernanz A, Gavira-Vallejo JM, Ruiz-Lopez JF (2006). Introduction to Raman microscopy of prehistoric rock paintings from the Sierra de las Cuerdas, Cuenca, Spain. *J. Raman Spectrosc.* 37:1054-1062.
- Kuzmanovski I, Trpkovska M, Soptrajanov B, Stefov V (1999). Target-testing factor analysis of Fourier transform infrared spectra as a tool for the determination of the composition of human urinary calculi. *Vibrat. Spectrosc.* 19:249-253.
- Lane MD (2007). Mid-infrared emission spectroscopy of sulfate and sulfate bearing minerals. *Am. Miner.* 92:1-18.
- Larson HH, Kerr PF (1963). Infrared Spectra, Symmetry and Structure Relations of some Carbonate Minerals. *Am. Miner.* P. 43.
- Madejova J, Komadel P (2001). Baseline Studies of the Clay Minerals Society Source Clays: Infrared Method. *Clays Clay Miner.* 49:410-432.
- Makreski P, Jovanovski G (2003). Mineral from Macedonia, Distinction between some Rhombohedral Carbonates by FTIR Spectroscopy. *Maced. Chem. Techno. Bull.* 22(1):25-32.
- Manjula K, Pazhanichamy K, Kumarans S, Evera T, Dalekeefe C and Rajendran K (2012). Growth Characterization of Calcium Oxalate Monohydrate Crystals Influenced *Costus Igneus* Aqueous Stem Extract. *Int. J. Pharm. Pharm. Sci.* P. 4.
- McCabe S, Smith BJ, Adamson C, Mullan D, McAlister J (2011). The "Greening" of Natural Stone Buildings: Quartz Sandstone Performance as a Secondary Indicator of Climate Change in the British Isles. *Atmos. Clim. Sci.* 1:165-171.
- Natali C, Beccaluva L, Bianchini G, Siena F (2011). Rhyolites associated to Ethiopian CFB: Clues for initial rifting at the Afar plume axis. *Earth Plan. Sci. Lett.* 312:59.
- Perez-Alonso M, Castro K, Martine-Arkarazo I, Angulo M, Olazabal MA, Madariaga JM (2004). Analysis of bulk and inorganic degradation products of stones, mortars and wall paintings by portable Raman microprobe spectroscopy. *Abstract, Anal. Bioanal. Chem.* 379(1):42.
- Pik R, Deniel C, Coulon C, Yirgu G, Hofmann C, Ayalew D (1998). The northwestern Ethiopian Plateau flood basalts: Classification and spatial distribution of magma types. *J. Volcan. Geotherm. Res.* 81:91.
- Plav B, Kobe S, Orel B (1999). Identification of Crystallization forms of CaCO₃ with FTIR Spectroscopy. *KZLTET* 33(6):517.
- Potgieter-Vermaak SS, Godoi RH, Grieken RV, Potgieter JH, Oujja M, Castillejo M (2005). Micro-structural characterization of black crust and laser cleaning of building stones by micro-Raman and SEM techniques. *Abstract, Spectrochim. Acta. Mol. Biomol. Spectrosc.* 61(11):2460.
- Ravisankar R, Annamalai GR, Rajan K, Naseerutheen A, Senthilkumar G (2012). Mineral Analysis in Archaeological Pottery from Porunthal, Dindigaldist, Tamilnadu, India by FTIR Spectroscopic Technique. *Int. J. Sci. Innov. Discov.* 2(1):53-60.
- Ravisankar R, Senthilkumar G, Kiruba S, Chandrasekaran A, Jebakumar PP (2010). Mineral analysis of coastal sediment samples of Tuna, Gujarat, India. *India J. Sci. Technol.* 3(7):858-862.
- Renzullia A, Antonellia F, Margottinib C, Santia P, Fratini F (2011). What kind of volcanite the rock-hewn churches of the Lalibela UNESCO's world heritage site are made of. *J. Cult. Herit.* 12:227-235.
- Ruffolo SA, Russa MF, Barca D, Casoli, Comite, Nava G, Crisci GM, Francesco AM, Miriello D (2010). Mineralogical, petrographic and chemical analyses for the study of the canvas "Cristo alla Colonna" from Cosenza, Italy: A case study. *Period. Mine. Spec.* pp. 71-79.
- Saikia BJ, Parthasarathy G (2010). Fourier Transform Infrared Spectroscopic Characterization of Kaolinite from Assam and Meghalaya, Northeastern India. *J. Mod. Phys.* 1:206-210.
- Saikia BJ, Parthasarathy G, Sarmahn C (2008). Fourier transform infrared spectroscopic estimation of crystallinity in SiO₂ based rocks. *Sci. Bull.* 31(5):775-779.
- Schiavon N (2007). Kaolinisation of granite in an urban environment.

- Environ. Geol. 52:399-407.
- Smith BJ, Gomez-Heras M, McCabe S (2008). Understanding the decay of stone-built cultural heritage. *Prog. Phys. Geog.* 32:439-461.
- Steven J (2005). Effect of environmental factors on the chemical weathering of plagioclase in Hawaiian basalt. *Phys. Geog.* 26(1):69-84.
- Valarmathi D, Abraham L, Gunasekaran S (2010). Growth of calcium oxalate monohydrate crystal by gel method and its spectroscopic analysis. *Indian J. Appl. Phys.* 48:36-38.
- Zanettin B (1992). Evolution of the Ethiopian Volcanic Province. *Mem. Lincee Sci. Fis. Nat.* 1:155.